PERIODICUM BIOLOGORUM
VOL. 127, No 3–4, 221–230, 2025
DOI: 10.18054/pb.v127i3-4.35802

UDC 57:61
CODEN PDBIAD
ISSN 0031-5362

Original research article

AGK2 pre-treatment mitigates hepatic ischemia--reperfusion injury by modulating sirtuin 2 expression and reducing inflammation and apoptosis

YINQIAN HE[1,#]
WEI LIU[2,#]
YAN ZHANG[3,*]

[1] Department of Neurological Rehabilitation, Xi'an International Medical Center Hospital, Xi'an, Shaanxi, China

[2] Department of Liver Disease, Yantai Qishan Hospital, Yantai, Shandong, China

[3] Department of Neurological Rehabilitation, Xi'an International Medical Center Hospital, Xi'an, Shaanxi, China

[#]Contributed equally.

***Correspondence:**
Yan Zhang
E-mail address: zhangyan126548@outlook.com

Keywords: AGK2; SIRT2; ischemia-reperfusion injury; NF-κB; Caspase-3

Abstract

Ischemia-reperfusion injury (IRI) significantly impacts liver surgeries and transplantation due to oxidative stress, inflammation, and apoptosis. This study examines the protective effects of 2-cyano-3-[5-(2,5-dichlorophenyl)-2-furanyl]-N-5-quinolinyl-2-propenamide (AGK2), a Sirtuin 2 (SIRT2) inhibitor, in hepatic IRI using in vitro and in vivo models. In vitro, HepG2 cells underwent hypoxia (1% oxygen for 45 minutes) followed by reoxygenation (21% oxygen for 2 hours) to simulate IRI. AGK2 was administered either 30 minutes before hypoxia (pre-treatment) or immediately after reoxygenation (post-treatment). Western blot analysis showed that IRI reduced SIRT2 expression to 50–60% of baseline levels, while AGK2 pre-treatment restored it to 130–150%, and post-treatment to 110–120%. Pre-treatment significantly reduced NF-κB activation and cleaved Caspase-3 levels, correlating with improved cell viability, as assessed by MTT assay. In vivo, a murine model of hepatic IRI (45 minutes ischemia, 2 hours reperfusion) was used, with AGK2 (20 mg/kg) administered pre- or post-treatment. IRI reduced hepatic SIRT2 expression to 50–60% of baseline, while AGK2 pre-treatment elevated it to 140–160%, and post-treatment to 110–130%. AGK2 pre-treatment significantly decreased NF-κB activation and cleaved Caspase-3 levels in liver tissues, indicating reduced inflammation and apoptosis. These findings suggest that AGK2 protects against hepatic IRI by modulating SIRT2 expression and attenuating inflammatory and apoptotic pathways. Pre-treatment consistently demonstrated superior efficacy compared to post-treatment, highlighting the importance of administration timing. This study supports the potential therapeutic application of AGK2 in mitigating hepatic ischemia-reperfusion injury.

Received March 30, 2025
Revised July 21, 2025
Accepted July 31, 2025

INTRODUCTION

Liver ischemia-reperfusion injury (IRI) remains a major clinical challenge in the context of liver transplantation, trauma, and hepatic resections *(1)*. IRI consists of an initial ischemic phase, characterized by a lack of oxygen and nutrient supply, followed by a reperfusion phase, during which the restoration of blood flow paradoxically exacerbates tissue damage *(2)*. The mechanisms underlying this damage include the overproduction of reactive oxygen species (ROS), activation of inflammatory pathways, and induction of hepatocyte apoptosis, leading to significant liver dysfunction *(3)*. Addressing these mechanisms is critical to reducing the morbidity and mortality associated with liver IRI.

Among the various molecular regulators implicated in liver IRI, Sirtuins 2 (SIRT2), a cytoplasmic member of the sirtuin family of Nicotinamide Adenine Dinucleotide (NAD+)-dependent deacetylases, has been identified as a key player *(4)*. SIRT2 is involved in the regulation of oxidative stress, inflammation, and cellular homeostasis *(4-6)*. Reduced SIRT2 expression during IRI is associated with increased oxidative stress, inflammation, and apoptosis *(7)*. Enhancing SIRT2 expression or activity may protect hepatocytes and mitigate the extent of injury.

NF-κB (nuclear factor kappa B), a master regulator of inflammation, is known to play a pivotal role in liver IRI by driving the transcription of pro-inflammatory cytokines *(8)*. Persistent activation of NF-κB contributes to the amplification of inflammatory responses and hepatocyte damage *(9)*. Strategies that suppress NF-κB activation while enhancing SIRT2 expression are promising therapeutic approaches to minimize liver damage during IRI.

2-cyano-3-[5-(2,5-dichlorophenyl)-2-furanyl]-N-5-quinolinyl-2-propenamide (AGK2), a selective inhibitor of SIRT2, has shown potential hepatoprotective effects under specific conditions by restoring cellular balance and modulating signaling pathways *(10-11)*. While AGK2 has primarily been studied as a SIRT2 modulator, its effects on oxidative stress and inflammation during liver IRI remain underexplored. In this study, we aim to investigate the role of AGK2 in modulating SIRT2 and NF-κB pathways to protect hepatocytes from IRI-induced damage.

The present study adopts a dual experimental model. Hepatocellular Carcinoma G2 (HepG2) cells are utilized to dissect the molecular mechanisms underlying AGK2's effects in vitro, providing an initial understanding of its influence on SIRT2 expression, NF-κB activity, apoptosis, and cell viability. After that, a murine model of liver IRI is employed to validate these findings in vivo, evaluating the impact of AGK2 on SIRT2 expression, NF-κB activity, and hepatocyte survival in a physiological context.

Our findings demonstrate the robust hepatoprotective effects of AGK2 against IRI through the modulation of SIRT2 and NF-κB pathways. AGK2 significantly enhanced SIRT2 expression, reduced NF-κB activation, and suppressed apoptosis, as observed in both HepG2 cells and a murine model. Furthermore, AGK2 improved cell viability in vitro and mitigated liver damage in vivo, emphasizing its therapeutic potential. These results provide compelling evidence for AGK2 as a promising candidate for the treatment of liver IRI, with its dual ability to combat oxidative stress and inflammation.

This study aims to elucidate AGK2's protective mechanisms by focusing on its dual modulation of SIRT2 and NF-κB. The findings will contribute to the development of novel therapeutic strategies for managing liver IRI and improving clinical outcomes in liver transplantation and surgical interventions.

MATERIALS AND METHODS

HepG2 model for IRI and AGK2 treatment

HepG2 Cell Culture

HepG2 cells were cultured in Dulbecco's Modified Eagle Medium (DMEM) supplemented with 10% fetal bovine serum (FBS), 1% penicillin-streptomycin, and maintained at 37°C in a humidified incubator with 5% Carbon dioxide (CO_2) *(12)*. All in vitro experiments were independently repeated at least three times (n = 3).

IRI simulation in HepG2 cells

To mimic ischemia-reperfusion conditions, cells were subjected to hypoxia for 45 minutes using a hypoxia chamber with 1% O_2, 5% CO_2, and 94% N_2 to simulate ischemia. For reperfusion, cells were reoxygenated by returning them to standard incubator conditions (37°C, 5% CO_2, and approximately 21% O_2) for 2 hours *(13)*.

AGK2 treatment in HepG2 cells

HepG2 cells were subjected to two treatment protocols to assess the effects of AGK2 under ischemia-reperfusion conditions. For pre-treatment, the cells were incubated with AGK2 (10 μM) for 30 minutes before the onset of ischemia. In the post-treatment protocol, AGK2 (10 μM) was added immediately following reperfusion. Control cells were maintained under standard atmospheric conditions (21% O_2, 5% CO_2, 37°C) without AGK2 treatment to serve as a baseline *(12-14)*. Each treatment condition was tested in triplicate and repeated in three independent experiments.

Sodium dodecyl sulfate-polyacrylamide gel electrophoresis (SDS PAGE) and western blot analysis

Protein extraction and immunoblotting

Liver tissues were homogenized in Radioimmunoprecipitation Assay buffer (RIPA) with protease inhibitors. Protein lysates from HepG2 cells were extracted using RIPA buffer containing protease inhibitors *(15)*. Equal amounts of protein (30 μg) were separated by SDS-PAGE and transferred to PVDF membranes. The membranes were probed with specific antibodies, including SIRT2 (1:1000, Cell Signaling Technology), NF-κB (p65) (1:1000, Cell Signaling Technology), and cleaved Caspase-3 (1:1000, Abcam). GAPDH (1:5000, Abcam) was used as a loading control. Protein bands were visualized using enhanced chemiluminescence (ECL) and subsequently quantified using ImageJ software. Western blotting was performed on samples from three independent biological replicates.

3-(4,5-dimethylthiazol-2-yl)-2,5-diphenyltetrazolium bromide (MTT) assay

Cell viability was assessed using the MTT assay. HepG2 cells were seeded in 96-well plates at a density of 10,000 cells per well. Following IRI and AGK2 treatments, the cells were incubated with an MTT solution (0.5 mg/mL) for 4 hours at 37°C. Formazan crystals formed during the assay were solubilized in DMSO, and the absorbance was measured at 570 nm using a microplate reader. Cell viability was then expressed as a percentage relative to the control group *(16)*. Each condition was tested in five technical replicates per experiment and repeated in three independent biological replicates (n = 3).

Animal model

Experimental animals

Male C57BL/6 mice (8–10 weeks old) were used. Mice were housed under standard conditions with ad libitum access to food and water. All procedures were approved by the Institutional Animal Care and Use Committee (IACUC).

Induction of liver IRI in mice

Male C57BL/6 mice (8–10 weeks old) were obtained from the Experimental Animal Center of Wuhan University. The mice were housed under standard conditions with ad libitum access to food and water. All experimental protocols were approved by the Institutional Animal Care and Use Committee (IACUC) and the Ethics Committee *(17)*.

Experimental groups

A total of 20 mice were used in the study, randomly divided into 4 experimental groups (n = 5 per group):

1. Control group (n = 5): No ischemia or reperfusion.
2. IRI group (n = 5): Mice subjected to liver IRI.
3. AGK2 pretreated group (n = 5): Mice pretreated with AGK2 (10 mg/kg) 30 minutes before ischemia.
4. AGK2 post-treated group (n = 5): Mice treated with AGK2 (10 mg/kg) immediately after reperfusion.

Each group contained 5 animals, and the experiment was performed once due to ethical considerations and animal usage constraints.

AGK2 treatment in mice

Pre-treatment involved intraperitoneal injection of AGK2 (10 mg/kg) 30 minutes before ischemia. Post-treatment was administered with AGK2 (10 mg/kg) immediately after reperfusion. Sham-operated mice underwent the same procedure without vascular occlusion.

Quantitative Real-Time PCR

Total RNA was extracted using TRIzol reagent and subsequently reverse-transcribed into cDNA. The gene expression levels of NF-κB and cleaved Caspase-3 were quantified using SYBR Green PCR Master Mix (Applied Biosystems) on a Real-Time PCR System, with GAPDH serving as the internal control *(18)*. Each sample was run in triplicate (technical replicates) and data are representative of three independent experiments (biological replicates).

Statistical Analysis

Data are presented as means ± standard deviation (SD). Statistical comparisons between multiple experimental groups were performed using one-way analysis of variance (ANOVA) followed by Tukey's post-hoc test for pairwise comparisons. For data that did not meet the assumptions of normality, non-parametric tests such as the Kruskal-Wallis test were applied. A p-value of less than 0.05 was considered statistically significant. All statistical analyses were performed using GraphPad Prism software (version 9). All quantitative data are based on at least three independent experimental repetitions unless otherwise specified.

RESULTS

AGK2 restores SIRT2 expression in HepG2 cells under IRI

To investigate the protective effects of AGK2 in IRI, an in vitro model using HepG2 cells was developed (Figure 1A). HepG2 cells, cultured under standard conditions in DMEM supplemented with 10% FBS, served as a reliable model for studying liver cell responses to oxidative stress and therapeutic interventions. The experimental workflow began with HepG2 cells maintained under standard atmospheric oxygen conditions (21% O_2, 5% CO_2, 37°C) conditions, representing the baseline state. Subsequently, ischemia was induced by placing cells in a hypoxic chamber with 1% oxygen for 45 minutes to mimic oxygen deprivation, a critical feature of IRI. Reperfusion followed, involving reoxygenation under standard atmospheric conditions (21% O_2) for 2 hours, simulating the restoration of blood flow and oxygen supply. Two distinct pathways were utilized to examine the timing of AGK2 intervention. In pre-treatment pathway, HepG2 cells were pretreated with AGK2 (10 μM) for 30 minutes before the induction of ischemia. This approach tested AGK2's protective potential when administered prophylactically. In post-treatment pathway, AGK2 was introduced immediately after reperfusion to evaluate its effectiveness in mitigating reperfusion-induced damage. The effects of AGK2 on ischemia-reperfusion were assessed by measuring the expression of SIRT2, a NAD+-dependent deacetylase implicated in cellular stress responses (Figure 1B). Western blot analysis revealed that SIRT2 expression in the control group was set as the reference value (100%) for comparative analysis. The IRI

group exhibited a marked reduction in SIRT2 expression, with levels decreasing to 50–60% of baseline (lane 1 vs. 2, $p < 0.001$), highlighting the impact of ischemic and reperfusion stress. AGK2 pre-treatment significantly restored SIRT2 expression, elevating it to 130–150% of baseline (lane 2 vs. 3, $p < 0.05$), suggesting enhanced stress response and cellular protection. AGK2 post-treatment moderately increased SIRT2 levels to 110–120%, indicating a partial recovery when the treatment was administered after the onset of reperfusion (lane 2 vs. 4, $p < 0.01$). A quantitative analysis normalized SIRT2 expression to GAPDH, demonstrating clear differences between groups (Figure 1C, $p < 0.05$). The bar graph in Figure 1C effectively illustrates these variations, emphasizing the superior efficacy of AGK2 pre-treatment in maintaining and enhancing SIRT2 levels compared to post-treatment. This data demonstrates the successful implementation of the HepG2 cell model for IRI and highlights AGK2's dual role as a pre- and post-treatment agent. The significant increase in SIRT2 expression following AGK2 pre-treatment underscores its potential for preemptive hepatoprotection in ischemic conditions. The significant increase in SIRT2 expression following AGK2 pre-treatment underscores its potential for preemptive hepatoprotection in ischemic conditions ($p < 0.05$).

AGK2 reduces NF-κB activation and apoptosis in HepG2 cells

Building upon the observed restoration of SIRT2 expression in HepG2 cells IRI (Figure 1), next we explored AGK2's impact on two critical downstream mediators of cellular stress: NF-κB (p65) and cleaved Caspase-3, which are central to inflammation and apoptosis, respectively. NF-κB is a key transcription factor activated during oxidative stress and inflammation. Under baseline conditions, NF-κB expression in HepG2 cells was low (100%, normalized to GAPDH). However, IRI led to a dramatic increase in NF-κB activation (lane 1 vs. 2, $p < 0.001$), with levels reaching approximately 200% of baseline, indicative of heightened inflammatory signaling. HepG2 cells pre-treated with AGK2 (10 μM) exhibited a significant reduction in NF-κB levels (lane 2 vs. 3, $p < 0.05$), suggesting robust inhibition of inflammatory signaling. This aligns with the previously observed enhancement of SIRT2 (Figure 1), which has been implicated in negatively regulating NF-κB activity. Post-treatment with AGK2 also reduced NF-κB activation but to a lesser extent (lane 2 vs. 4, $p < 0.01$). NF-κB expression levels were restored to 90–100% of baseline. While this indicates partial inhibition of inflammation, the effect was less pro-

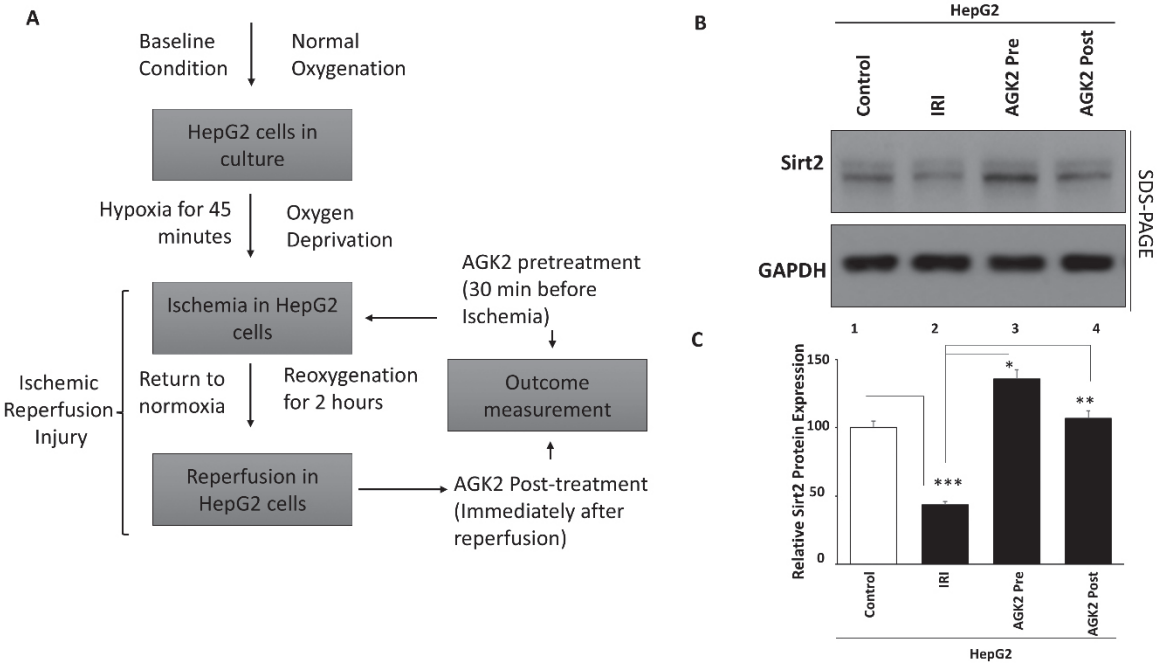

Figure 1. ***Experimental design and analysis of AGK2 treatment in HepG2 cells under Liver ischemia-reperfusion injury (IRI).*** *(**A**) Experimental workflow for simulating IRI in HepG2 cells. HepG2 cells were cultured under standard conditions and subjected to hypoxia (1% O_2, 5% CO_2, 94% N_2) for 45 minutes to induce ischemia, followed by reoxygenation (21% O_2, 5% CO_2) for 2 hours to simulate reperfusion. (**B**) Western blot analysis of SIRT2 expression in HepG2 cells. HepG2 cells were subjected to four experimental conditions: mock (control), IRI, AGK2 pre-treatment (10 μM for 30 minutes before ischemia), and AGK2 post-treatment (10 μM immediately after reperfusion). SIRT2 expression was evaluated by Western blotting. (**C**) Quantification of SIRT2 expression levels in HepG2 cells under various conditions. Protein expression of SIRT2 was assessed by Western blotting, and the relative levels were normalized to GAPDH. Data are expressed as mean ± SD from three independent experiments. * for $p<0.05$, ** $p<0.01$, *** $p<0.001$ compared to IRI group.* ***Lane 1:*** *Control,* ***Lane 2:*** *IRI,* ***Lane 3:*** *AGK2 pre-treatment,* ***Lane 4:*** *AGK2 post-treatment.*

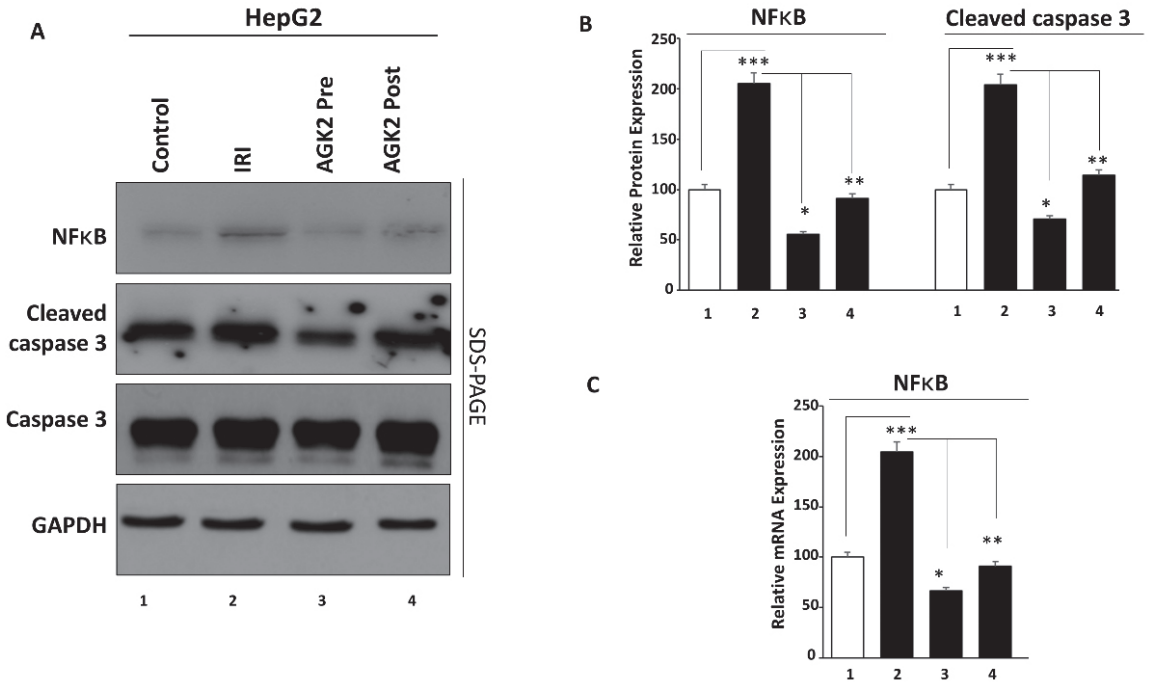

Figure 2. ***AGK2 Reduces Nuclear Factor Kappa B (NF-κB) Activation and Apoptosis in HepG2 Cells Under Liver ischemia-reperfusion injury IRI.*** *(**A**) Western blot images illustrating the expression levels of NF-κB (p65) and cleaved Caspase-3 in HepG2 cells under different experimental conditions, including control, IRI, AGK2 pre-treatment, and AGK2 post-treatment. GAPDH serves as the loading control. (**B**) Quantitative representation of NF-κB and cleaved Caspase-3 protein levels normalized to GAPDH, derived from densitometric analysis of western blot results. Groups include control, IRI, AGK2 pre-treatment, and AGK2 post-treatment. (**C**) Real-time PCR analysis showing mRNA expression levels of NF-κB in HepG2 cells across experimental groups. Data are normalized to GAPDH and presented as fold changes relative to the control. Data are expressed as mean ± SD from three independent experiments. * for p<0.05, ** p<0.01, *** p<0.001 compared to IRI group.* ***Lane 1:*** *Control,* ***Lane 2:*** *IRI,* ***Lane 3:*** *AGK2 pre-treatment,* ***Lane 4:*** *AGK2 post-treatment.*

nounced than that of pre-treatment, further emphasizing the importance of timely AGK2 administration.

Caspase-3, a critical effector of apoptosis, was similarly evaluated to assess AGK2's role in mitigating cell death. Cleaved Caspase-3 expression in the control group was used as the baseline reference (100%, normalized to GAPDH) for comparative analysis. In response to IRI, Caspase-3 activation significantly increased, reaching 180–200% of baseline, indicating a substantial apoptotic response (lane 1 vs. 2, $p < 0.001$). AGK2 pre-treatment resulted in a marked reduction in cleaved Caspase-3 levels, bringing them down to 60–70% of baseline (lane 2 vs. 3, $p < 0.05$). This substantial decrease suggests that AGK2 effectively inhibits apoptotic pathways when administered prophylactically, correlating with the restoration of SIRT2 observed in Figure 1. Post-treatment with AGK2 also reduced Caspase-3 levels, albeit to a lesser degree, with levels decreasing to 80–90% of baseline (lane 2 vs. 4, $p < 0.01$). This partial reduction underscores AGK2's potential in limiting apoptosis even when administered after ischemic stress but highlights the greater efficacy of pre-treatment.

The quantitative graph (Figure 2B) clearly illustrates these differences ($p < 0.05$), highlighting AGK2's dose- and timing-dependent effects on NF-κB activity and cleaved caspase 3.

Quantitative analysis (Figure 2C) and real-time PCR data further validate these observations ($p < 0.05$), confirming AGK2's role in attenuating apoptosis at the transcriptional and protein levels.

Our data demonstrates that AGK2 reduces NF-κB activation and Caspase-3-mediated apoptosis in HepG2 cells subjected to IRI. The data suggest a dual role for AGK2 in attenuating both inflammatory and apoptotic pathways, with pre-treatment consistently providing the most pronounced protective effects. These findings further support AGK2's potential as a therapeutic agent in ischemic liver injury.

AGK2 improves cell viability in HepG2 cells under IRI

To evaluate the protective effects of AGK2 on overall cellular health, the viability of HepG2 cells subjected to IRI was assessed using an MTT assay (Figure 3). This assay measures metabolic activity as an indicator of cell survival and function. Under baseline (control) conditions, cell viability was set at 100%, reflecting optimal metabolic function and the absence of cellular stress.

However, the induction of IRI significantly compromised cell viability, reducing it to 50–60% of the control levels ($p < 0.001$). This reduction highlights the profound impact of hypoxia and subsequent reoxygenation on hepatocyte survival. Cells pre-treated with AGK2 (10 μM) demonstrated a remarkable improvement in viability. The MTT assay revealed that pre-treatment restored cell viability to 85–90% of control levels ($p < 0.01$), indicating substantial protection against IRI-induced damage. These findings align with the enhanced SIRT2 expression (Figure 1) and reduced NF-κB activation and apoptosis (Figure 2) observed in AGK2-pre-treated cells, suggesting a consistent protective mechanism. Post-treatment with AGK2 also improved cell viability, albeit to a lesser extent than pre-treatment. The viability of post-treated cells increased to 70–80% of control levels ($p < 0.05$). While this improvement indicates AGK2's ability to mitigate some of the damage caused by reperfusion, the reduced efficacy compared to pre-treatment further emphasizes the importance of intervention timing in protecting cells from IRI.

This data underscores AGK2's capacity to improve cell viability in HepG2 cells subjected to IRI. The data demonstrate that pre-treatment with AGK2 provides near-complete protection against IRI-induced metabolic dysfunction, while post-treatment offers moderate rescue effects. These findings align with the broader mechanistic insights presented in Figures 1 and 2, further supporting AGK2's potential as a therapeutic intervention for ischemic liver injury.

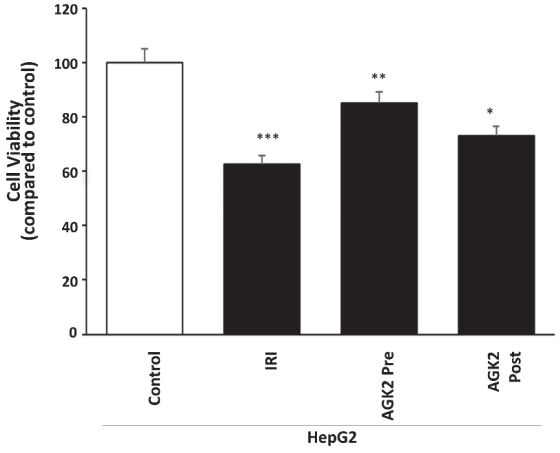

Figure 3. ***AGK2 Improves Cell Viability in HepG2 Cells Under IRI.*** *Bar graph illustrating the viability of HepG2 cells assessed using the MTT assay under various experimental conditions: control (baseline), IRI, AGK2 pre-treatment, and AGK2 post-treatment. Cell viability is expressed as a percentage relative to the control group. AGK2 pre-treatment demonstrates a significant protective effect, restoring cell viability to near-baseline levels, while post-treatment provides moderate rescue effects. Data are expressed as mean ± SD from three independent experiments. * for p<0.05, ** p<0.01, *** p<0.001 compared to control group.* ***Lane 1:*** *Control,* ***Lane 2:*** *IRI,* ***Lane 3:*** *AGK2 pre-treatment,* ***Lane 4:*** *AGK2 post-treatment.*

AGK2 restores SIRT2 expression in a murine model of IRI

To evaluate the protective role of AGK2 in a physiologically relevant context, a murine model of IRI was employed. This model mimicked hepatic IRI through temporary occlusion of hepatic blood flow (ischemia) followed by restoration (reperfusion) (Figure 4A). The impact of AGK2 on hepatic SIRT2 expression was assessed under different treatment regimens. In the sham group, where no ischemia or reperfusion was induced, SIRT2 expression (Figure 4B) was maintained at baseline levels (100%, normalized to GAPDH). However, in the IRI group, hepatic ischemia (45 minutes) followed by reperfusion (2 hours) resulted in a significant decrease in SIRT2 expression, with levels falling to 50–60% of the baseline (lane 1 vs. 2, $p < 0.001$). This reduction reflects the deleterious effects of oxidative stress and inflammation caused by IRI on hepatocyte function. Mice pre-treated with AGK2 (20 mg/kg) 30 minutes prior to ischemia induction demonstrated a robust increase in SIRT2 expression. SIRT2 levels were significantly restored, reaching 140–160% of baseline (lane 2 vs. 3, $p < 0.01$). This enhancement indicates a strong protective effect of AGK2 against ischemic stress, consistent with its effects observed in the HepG2 cell model (Figures 1–3). The pre-treatment results further emphasize the therapeutic advantage of prophylactic AGK2 administration in mitigating IRI-induced damage. In the post-treatment group, AGK2 was administered immediately after the onset of reperfusion. Western blot analysis revealed a moderate recovery of SIRT2 levels, with expression increasing to 110–130% of baseline (lane 2 vs. 4, $p < 0.05$). Although less effective than pre-treatment, this recovery suggests that AGK2 retains the ability to partially restore SIRT2 expression even when applied after ischemic damage has occurred.

These quantitative findings (Figure 4C) corroborate the trends observed in the western blot data, reinforcing the protective role of AGK2 against IRI-induced suppression of SIRT2 ($p < 0.05$).

Our data shows that AGK2 significantly restores SIRT2 expression in a murine model of IRI injury. Pre-treatment with AGK2 consistently yields superior outcomes, with marked restoration of SIRT2 expression, while post-treatment offers moderate recovery. These findings, together with the in vitro results, strongly support AGK2's potential as a therapeutic agent for mitigating hepatic IRI.

AGK2 reduces NF-κB activation and apoptosis in murine liver tissues

To further investigate AGK2's protective mechanisms in IRI, its effects on NF-κB activation and apoptosis in murine liver tissues were assessed. Building on prior results demonstrating SIRT2 restoration (Figure 4) and its downstream effects on inflammation and apoptosis in HepG2 cells (Figures 2 and 3), this figure evaluates AGK2's in vivo modulation of NF-κB a nd cleaved Cas-

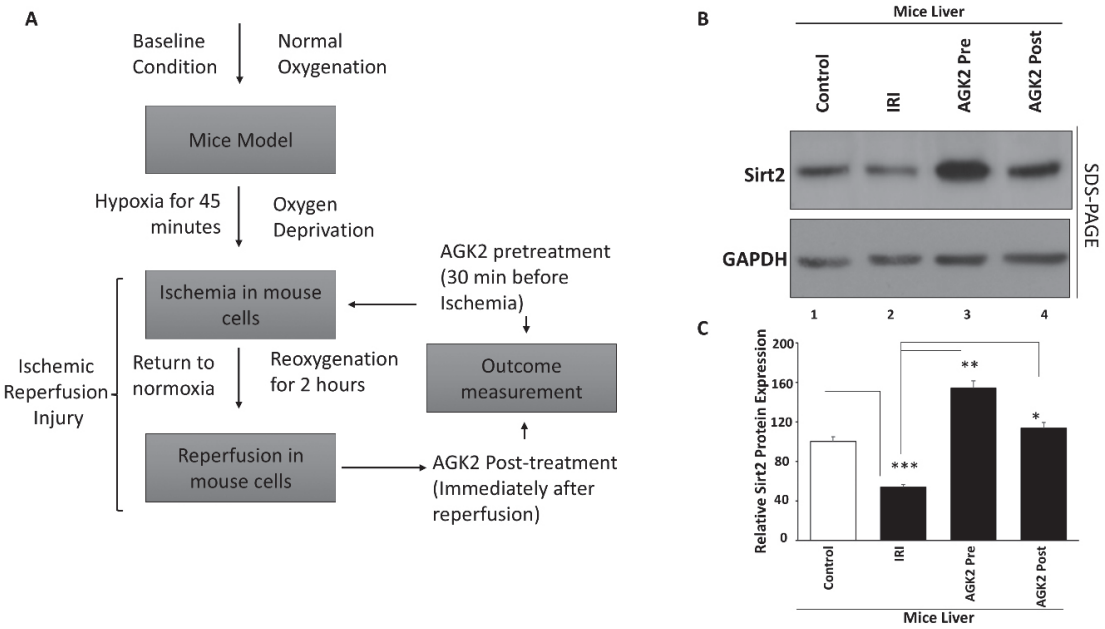

Figure 4. ***AGK2 restores SIRT2 expression in a murine model of IRI.*** *(**A**) Diagram depicting the murine model of IRI and AGK2 treatment protocols. Experimental conditions include sham (no IRI), IRI, AGK2 pre-treatment (administered 30 minutes before ischemia), and AGK2 post-treatment (administered immediately after reperfusion). (**B**) Western blot analysis showing SIRT2 expression in murine liver tissues under different experimental conditions. GAPDH was used as a loading control. (**C**) Quantitative graph representing SIRT2 expression levels normalized to GAPDH across the experimental groups. Data reflect the effects of IRI and AGK2 treatment on SIRT2 expression in murine liver tissues. Data are expressed as mean ± SD from three independent experiments. * for p<0.05, ** p<0.01, *** p<0.001 compared to IRI group.* ***Lane 1:*** *Control,* ***Lane 2:*** *RI,* ***Lane 3:*** *AGK2 pre-treatment,* ***Lane 4:*** *AGK2 post-treatment.*

pase-3—key mediators of inflammatory and apoptotic responses.NF-κB, a central regulator of inflammation, was significantly activated following IRI. Western blot analysis (Figure 5A) revealed that NF-κB expression was maintained at baseline levels (lane 1). A marked increase in NF-κB levels was observed (lane 1 vs. 2, p < 0.001),

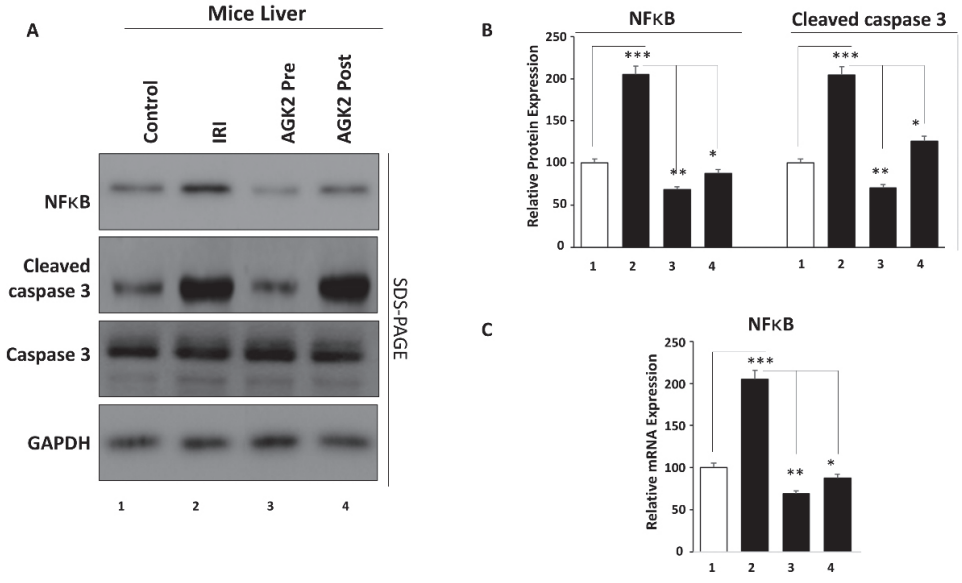

Figure 5. ***AGK2 Attenuates NF-κB Activation and Apoptosis in Murine Liver Tissues Following IRI.*** *(**A**) Western blot analysis of NF-κB expression in liver tissues from mice subjected to IRI, with or without AGK2 treatment (pre- or post-treatment). (**B**) Quantitative analysis of NF-κB and cleaved Caspase-3 levels normalized to GAPDH. (**C**) Real-time PCR analysis showing the effect of AGK2 on NF-κB in liver tissues. The data assess AGK2's potential to modulate inflammatory and apoptotic pathways in the context of IRI. Data are expressed as mean ± SD from three independent experiments. * for p<0.05, ** p<0.01, *** p<0.001 compared to IRI group.* ***Lane 1:*** *Control,* ***Lane 2:*** *RI,* ***Lane 3:*** *AGK2 pre-treatment,* ***Lane 4:*** *AGK2 post-treatment.*

consistent with the induction of a pro-inflammatory state caused by oxidative stress during reperfusion. Mice pre-treated with AGK2 (20 mg/kg) showed a significant reduction in NF-κB activation, (lane 2 vs. 3, $p < 0.01$). This parallels the reduction in NF-κB observed in HepG2 cells (Figure 2), further supporting the hypothesis that AGK2's upregulation of SIRT2 inhibits NF-κB-mediated inflammation. AGK2 post-treatment moderately reduced NF-κB levels, (lane 2 vs. 4, $p < 0.05$). While less effective than pre-treatment, this outcome suggests that AGK2 retains partial efficacy in dampening inflammatory responses when administered after ischemic insult. Caspase-3, a key effector of apoptosis, was also evaluated to assess AGK2's role in reducing cell death in vivo. Cleaved Caspase-3 levels, indicative of apoptotic activity also showed the same trends as NF-κB levels ($p < 0.05$).

Quantitative graphs of NF-κB/GAPDH and cleaved Caspase-3/GAPDH levels (Figure 5B) and real-time PCR analysis (Figure 5C) confirm these trends ($p < 0.05$), showing clear suppression of NF-κB and apoptotic markers in AGK2-treated group. Our data highlights AGK2's ability to suppress NF-κB activation and cleaved Caspase-3 levels in murine liver tissues, further confirming its protective effects against IRI. Pre-treatment consistently outperforms post-treatment, emphasizing the importance of early intervention. These results, in conjunction with Figures 1–4, underscore AGK2's therapeutic potential in mitigating the inflammatory and apoptotic consequences of IRI injury.

DISCUSSION

IRI remains a significant challenge in clinical settings, particularly in liver transplantation and hepatic surgeries *(19)*. The dual-phase insult of hypoxia followed by oxidative stress during reoxygenation triggers complex molecular pathways involving inflammation, oxidative stress, and apoptosis, leading to extensive tissue damage *(20)*. This study investigated the potential protective effects of AGK2, a SIRT2 inhibitor, in both in vitro (HepG2 cells) and in vivo (murine) models of hepatic IRI. Our findings demonstrate that AGK2 treatment, particularly when administered as a pre-treatment, effectively mitigates IRI-induced damage by enhancing SIRT2 expression, reducing NF-κB activation, and suppressing apoptosis. These results highlight AGK2's potential as a therapeutic agent for managing hepatic IRI.

Our data indicate that AGK2 significantly restores SIRT2 expression in both HepG2 cells and murine liver tissues subjected to IRI. Pre-treatment with AGK2 consistently resulted in greater restoration of SIRT2 levels compared to post-treatment. This aligns with previous studies that highlight the protective role of SIRT2 in oxidative stress and metabolic homeostasis *(4)*. SIRT2 is known to modulate inflammatory and apoptotic pathways by deacetylating key substrates, including NF-κB, which suggests that its restoration is central to AGK2's protective effects.

However, some studies have reported conflicting roles of SIRT2 in IRI. For example, Wang et al. observed that SIRT2 inhibition exacerbated oxidative stress in cardiac IRI, highlighting tissue-specific responses to SIRT2 modulation *(21)*. This suggests that AGK2's protective effects in hepatic IRI may reflect unique liver-specific regulatory mechanisms. Further research is required to delineate these tissue-specific roles.

NF-κB is a master regulator of inflammation and a critical mediator of IRI-induced damage. In this study, IRI led to a significant increase in NF-κB activation in both HepG2 cells and murine liver tissues, consistent with its established role in promoting pro-inflammatory cytokine expression *(22)*. AGK2 treatment, particularly as a pre-treatment, significantly reduced NF-κB activation, likely through its upregulation of SIRT2.

These findings align with reports that SIRT2 negatively regulates NF-κB signaling by deacetylating the p65 subunit, thereby suppressing its transcriptional activity *(23)*. In contrast, post-treatment with AGK2 showed moderate reductions in NF-κB levels, underscoring the importance of timing in mitigating inflammatory responses. This is consistent with the idea that pre-treatment allows for the establishment of a protective cellular environment before the onset of oxidative stress.

Caspase-3 activation is a hallmark of apoptotic cell death in IRI *(24)*. Our results show that IRI significantly increased cleaved Caspase-3 levels in both HepG2 cells and murine liver tissues, consistent with previous reports of apoptosis as a major contributor to hepatocellular injury during IRI *(25)*. AGK2 treatment markedly suppressed cleaved Caspase-3 levels, particularly when administered as a pre-treatment, highlighting its anti-apoptotic effects.

These findings are supported by studies demonstrating that SIRT2 activation reduces mitochondrial dysfunction and inhibits Caspase-3-mediated apoptosis *(26)*. However, the moderate effects observed with AGK2 post-treatment suggest that while intervention after reperfusion can reduce apoptosis, it may not fully reverse the damage initiated during ischemia.

One of the most critical findings of this study is the superior efficacy of AGK2 pre-treatment compared to post-treatment in mitigating IRI-induced damage. Pre-treatment enhanced SIRT2 expression, reduced NF-κB activation, and suppressed apoptosis more effectively than post-treatment across both models. These results are consistent with the notion that early intervention allows for the establishment of protective mechanisms before the onset of oxidative stress. Post-treatment, while still effec-

tive, is likely limited by the extent of irreversible damage that occurs during ischemia.

The findings of this study provide strong evidence for AGK2's potential as a therapeutic agent for hepatic IRI. However, there are several limitations to consider. First, the study used a single dose of AGK2, and dose-response studies are needed to optimize its therapeutic efficacy. Second, while the murine model provides valuable insights, translation to human IRI requires validation in clinical trials. Additionally, the specific downstream targets of SIRT2 modulation by AGK2 remain to be elucidated.

CONCLUSION

This study demonstrates that AGK2 provides robust protection against hepatic IRI by enhancing SIRT2 expression, reducing NF-κB activation, and suppressing apoptosis. The superior efficacy of pre-treatment emphasizes the importance of early intervention in managing IRI. These findings contribute to the growing body of evidence supporting SIRT2 modulation as a promising therapeutic strategy. Future studies should focus on clinical validation and exploring AGK2's potential in other organ systems affected by IRI.

REFERENCES

1. ELTZSCHIG H and ECKLE T 2011 Ischemia and reperfusion-from mechanism to translation. Nat Med 17: 1391-1401. https://doi.org/10.1038/nm.2507
2. COWLED P and FITRIDGE R 2011 Pathophysiology of reperfusion injury. In: FITRIDGE R and THOMPSON M (Eds) Mechanisms of Vascular Disease: A Reference Book for Vascular Specialists, University of Adelaide Press, Adelaide (AU), Ch. 18 https://doi.org/10.1017/UPO9781922064004
3. ALLAMEH A, NIAYESH-MEHR R, ALIARAB A, SEBASTIANI G and PANTOPOULOS K 2023 Oxidative stress in liver pathophysiology and disease. Antioxidants (Basel) 12(9): 1653. https://doi.org/10.3390/antiox12091653
4. ZHU C, DONG X, WANG X, ZHENG Y, QIU J, PENG Y, XU J, CHAI Z and LIU C 2022 Multiple roles of SIRT2 in regulating physiological and pathological signal transduction. Genet Res (Camb) 2022: 9282484. https://doi.org/10.1155/2022/9282484
5. LIN J, SUN B, JIANG C, HONG H and ZHENG Y 2013 Sirt2 suppresses inflammatory responses in collagen-induced arthritis. Biochem Biophys Res Commun 441(4): 897-903. https://doi.org/10.1016/j.bbrc.2013.10.153
6. REN Y R, YE Y L, FENG Y, et al. 2021 SL010110, a lead compound, inhibits gluconeogenesis via SIRT2-p300-mediated PEPCK1 degradation and improves glucose homeostasis in diabetic mice. Acta Pharmacol Sin 42(11): 1834-1846. https://doi.org/10.1038/s41401-020-00609-w
7. KAITSUKA T, MATSUSHITA M and MATSUSHITA N 2021 Regulation of hypoxic signaling and oxidative stress via the microRNA-SIRT2 axis and its relationship with aging-related diseases. Cells 10(12): 3316. https://doi.org/10.3390/cells10123316
8. LIU T, ZHANG L and JOO D 2017 NF-κB signaling in inflammation. Signal Transduct Target Ther 2: 17023. https://doi.org/10.1038/sigtrans.2017.23
9. HAYDEN M S and GHOSH S 2012 NF-κB, the first quarter-century: remarkable progress and outstanding questions. Genes Dev 26(3): 203-234. https://doi.org/10.1101/gad.183434.111
10. YU H B, JIANG H, CHENG S T, HU Z W and REN J H 2018 AGK2, a SIRT2 inhibitor, inhibits hepatitis B virus replication in vitro and in vivo. Int J Med Sci 15(12): 1356-1364. https://doi.org/10.7150/ijms.26125
11. PIRACHA Z Z, KWON H, SAEED U, KIM J, JUNG J, CHWAE Y J, PARK S, SHIN H J and KIM K 2018 Sirtuin 2 isoform 1 enhances hepatitis B virus RNA transcription and DNA synthesis through the AKT/GSK-3*β*/*β*-catenin signaling pathway. J Virol 92(21): e00955-18. https://doi.org/10.1128/jvi.00955-18
12. SAEED U, KIM J, PIRACHA Z Z, KWON H, JUNG J, CHWAE Y J, PARK S, SHIN H J and KIM K 2019 Parvulin 14 and Parvulin 17 bind to HBx and cccDNA and upregulate hepatitis B virus replication from cccDNA to virion in an HBx-dependent manner. J Virol 93(6): e01840-18. https://doi.org/10.1128/jvi.01840-18
13. CHEN T and VUNJAK-NOVAKOVIC G 2018 In vitro models of ischemia-reperfusion injury. Regen Eng Transl Med 4(3): 142-153. https://doi.org/10.1007/s40883-018-0056-0
14. PIRACHA Z Z, SAEED U, PIRACHA I E, NOOR S and NOOR E 2024 Decoding the multifaceted interventions between human sirtuin 2 and dynamic hepatitis B viral proteins to confirm their roles in HBV replication. Front Cell Infect Microbiol 13: 1234903. https://doi.org/10.3389/fcimb.2023.1234903
15. PIRACHA Z Z, SAEED U, KIM J, KWON H, CHWAE Y J, LEE H W, LIM J H, PARK S, SHIN H J and KIM K 2020 An alternatively spliced sirtuin 2 isoform 5 inhibits hepatitis B virus replication from cccDNA by repressing epigenetic modifications made by histone lysine methyltransferases. J Virol 94(16): e00926-20. https://doi.org/10.1128/JVI.00926-20
16. SAEED U and PIRACHA Z Z 2023 PIN1 and PIN4 inhibition via parvulin impeders Juglone, PiB, ATRA, 6,7,4′-THIF, KPT6566, and EGCG thwarted hepatitis B virus replication. Front Microbiol 14: 921653. https://doi.org/10.3389/fmicb.2023.921653
17. ABE Y, HINES I N, ZIBARI G, PAVLICK K, GRAY L, KITAGAWA Y and GRISHAM M B 2009 Mouse model of liver ischemia and reperfusion injury: method for studying reactive oxygen and nitrogen metabolites in vivo. Free Radic Biol Med 46(1): 1-7. https://doi.org/10.1016/j.freeradbiomed.2008.09.029
18. SAEED U, PIRACHA Z Z and MANZOOR S 2017 Hepatitis C virus induces oxidative stress and DNA damage by regulating DNAPKCs, ATM, ATR and PARP mediated signaling and guards cell from cancerous condition by upregulating RB, P53 and down-regulating VEGF. Acta Virol 61(3): 316-323. https://doi.org/10.4149/av_2017_310
19. DAR W A, SULLIVAN E, BYNON J S, ELTZSCHIG H and JU C 2019 Ischaemia reperfusion injury in liver transplantation: cellular and molecular mechanisms. Liver Int 39(5): 788-801. https://doi.org/10.1111/liv.14091
20. COIMBRA-COSTA D, ALVA N, DURAN M, CARBONELL T and RAMA R 2017 Oxidative stress and apoptosis after acute respiratory hypoxia and reoxygenation in rat brain. Redox Biol 12: 216-225. https://doi.org/10.1016/j.redox.2017.02.014
21. WANG Y, YANG J, HONG T, CHEN X and CUI L 2019 SIRT2: Controversy and multiple roles in disease and physiology. Ageing Res Rev 55: 100961. https://doi.org/10.1016/j.arr.2019.100961
22. ANILKUMAR S and WRIGHT-JIN E 2024 NF-κB as an inducible regulator of inflammation in the central nervous system. Cells 13(6): 485. https://doi.org/10.3390/cells13060485
23. ROTHGIESSER K M, ERENER S, WAIBEL S, LÜSCHER B and HOTTIGER M O 2010 SIRT2 regulates NF-κB-dependent gene expression through deacetylation of p65 Lys310. J Cell Sci 123(24): 4251-4258. https://doi.org/10.1242/jcs.073783

24. CHOUDHARY G S, AL-HARBI S and ALMASAN A 2015 Caspase-3 activation is a critical determinant of genotoxic stress-induced apoptosis. Methods Mol Biol 1219: 1-9. https://doi.org/10.1007/978-1-4939-1661-0_1

25. PRETZSCH E, NIEß H, KHALED N B, BÖSCH F, GUBA M, WERNER J, ANGELE M and CHAUDRY I H 2022 Molecular mechanisms of ischaemia-reperfusion injury and regeneration in the liver-shock and surgery-associated changes. Int J Mol Sci 23(21): 12942. https://doi.org/10.3390/ijms232112942

26. CHA Y, KIM T, JEON J, JANG Y, KIM P B, LOPES C, LEBLANC P, COHEN B M and KIM K S 2021 SIRT2 regulates mitochondrial dynamics and reprogramming via MEK1-ERK-DRP1 and AKT1-DRP1 axes. Cell Rep 37(13): 110155. https://doi.org/10.1016/j.celrep.2021.110155